



UNIVERSITY OF LEEDS

This is a repository copy of *Responsivity of quantum well infrared photodetectors at terahertz detection wavelengths* .

White Rose Research Online URL for this paper:
<http://eprints.whiterose.ac.uk/1685/>

Article:

Gadir, M.A., Harrison, P. and Soref, R.A. (2002) Responsivity of quantum well infrared photodetectors at terahertz detection wavelengths. *Journal of Applied Physics*, 91 (9). pp. 5820-5825. ISSN 1089-7550

<https://doi.org/10.1063/1.1467951>

Reuse

See Attached

Takedown

If you consider content in White Rose Research Online to be in breach of UK law, please notify us by emailing eprints@whiterose.ac.uk including the URL of the record and the reason for the withdrawal request.



eprints@whiterose.ac.uk
<https://eprints.whiterose.ac.uk/>

Responsivity of quantum well infrared photodetectors at terahertz detection wavelengths

M. A. Gadir^{a)} and P. Harrison

IMP, School of Electronic and Electrical Engineering, The University of Leeds, LS2 9JT United Kingdom

R. A. Soref

Sensors Directorate, AFRL/SNHC, Air Force Research Laboratory, Hanscom Air Force Base, Massachusetts 01731

(Received 18 October 2001; accepted for publication 18 February 2002)

A first-principles model of the photocurrent in quantum well infrared photodetectors (QWIPs) is derived. The model examines the responsivity, carrier capture probability and quantum efficiency. It is found that the QWIP sensitivity reaches a plateau below the 10 μm detection wavelength and remains nearly constant from 10 to 50 μm. © 2002 American Institute of Physics.

[DOI: 10.1063/1.1467951]

I. INTRODUCTION

Quantum well infrared photodetectors (QWIPs) have attracted the attention of many researchers during the last decade,¹⁻⁴ and the detailed physical understanding of QWIP operation has stimulated study of optimum QWIP design. This has resulted in the proposal of several theoretical models⁵⁻⁸ to express primary QWIP characteristics such as responsivity, detectivity, photoconductive gain and photocurrent. However, the QWIP formulas derived from these different models vary due to the diversity in definitions and basic assumptions.

In this article, a simplified unifying model is presented with the aid of some of the definitions and assumptions from the models mentioned before. It starts by defining the photocurrent in a simple detector and linking the physical characteristics of capture probability, gain, and ultimately the responsivity, to the detection wavelength. The aim is to understand the consequences on the photocurrent of extending the detection wavelength of QWIPs to their far-infrared or terahertz limits.

II. PHOTOCURRENT AND PHOTOCONDUCTIVE GAIN

Figure 1 shows a simple schematic diagram of a detector,⁹ where L is the thickness and A_d is the surface area of a slab of photoconductive material, and Φ_s is the optical flux incident normally. The intensity of the flux is usually taken to decrease exponentially with the penetrating depth z ,⁹ hence, the intensity of flux at any depth z is

$$\Phi(z) = \Phi_s(1-r)\exp(-\alpha z),$$

where r is the reflection coefficient of the surface and α is the absorption coefficient of the material.

The photocarrier generation rate per unit volume is given by⁹

$$G(z) = -\frac{1}{A_d} \frac{d\Phi(z)}{dz},$$

$$\therefore G(z) = \frac{\alpha}{A_d} \Phi_s(1-r)\exp(-\alpha z).$$

At steady state the photogenerated carrier density $P(z)$ is constant i.e.,

$$\frac{\partial P(z)}{\partial t} = 0,$$

hence, the generation rate must be equal to the recombination rate. Say the latter is described by a recombination lifetime τ , then

$$\frac{\partial P(z)}{\partial t} = G(z) - \frac{P(z)}{\tau} = 0,$$

and hence

$$P(z) = \tau G(z).$$

The average photoelectron density is therefore

$$\begin{aligned} \bar{P} &= \frac{1}{L} \int_0^L P(z) dz = \frac{1}{L} \int_0^L G(z) \tau dz \\ &= \frac{\Phi_s \tau}{\alpha L A_d} (1-r) \int_0^L \exp(-\alpha z) dz, \end{aligned}$$

$$\therefore \bar{P} = \frac{\Phi_s \tau}{L A_d} (1-r) [1 - \exp(-\alpha L)] = \eta \frac{\Phi_s \tau}{L A_d},$$

where η is known as the quantum efficiency and is defined here as the probability that a photon is absorbed in a quantum well to produce a photoexcited electron. This quantum well efficiency is shown later

$$\eta = (1-r) [1 - \exp(-\alpha l_w)], \tag{1}$$

where the absorbing length L is now taken as the width l_w of the quantum well.¹⁰ Thus, αl_w . Recalling that a general current density is of the form “ nev ,” then the photocurrent

$$I_p = \bar{P} e v A_d \Rightarrow I_p = (\eta \Phi_s) e \frac{\tau v}{L},$$

^{a)}Electronic mail: eenmag@leeds.ac.uk

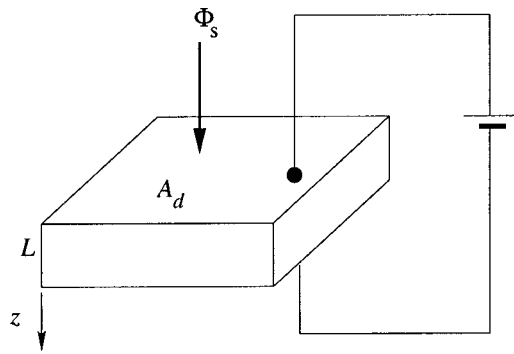


FIG. 1. The geometry of a detector.

thus

$$I_p = e\Phi_s \eta g, \tag{2}$$

where g is known as the photocurrent gain and can be interpreted as the ratio of the electron mean free path τv to the sample thickness L and is interpreted as a measure of the photoelectron transport.^{9,11} The photoconductive gain is viewed in terms of a quantum well capture probability P_c and is derived from Fig. 2, see Refs. 7 and 10.

The total photocurrent consists of the remaining photocurrent (i.e., electrons not captured by the well) $(1 - P_c)I_p$ and the emitted current from the well $(1 - P_c)i_p$,¹⁰ see Fig. 2. In order to maintain current continuity

$$I_p = (1 - P_c)I_p + (1 - P_c)i_p,$$

$$\therefore I_p P_c = (1 - P_c)i_p$$

after using the definition in Eq. (2), I_p and i_p become¹⁰

$$I_p = e\Phi_s \eta_n g \text{ and } i_p = e\Phi_s \eta,$$

where η_n is the quantum efficiency of a number N of wells in a QWIP, and η is the quantum efficiency of a single well with unit gain. Now $P_c I_p = (1 - P_c)i_p$, therefore

$$e\Phi_s \eta_n g P_c = (1 - P_c)e\Phi_s \eta,$$

$$\therefore g = \frac{1 - P_c}{P_c} \frac{\eta}{\eta_n}.$$

Recalling that $\eta_n = \eta N$, then

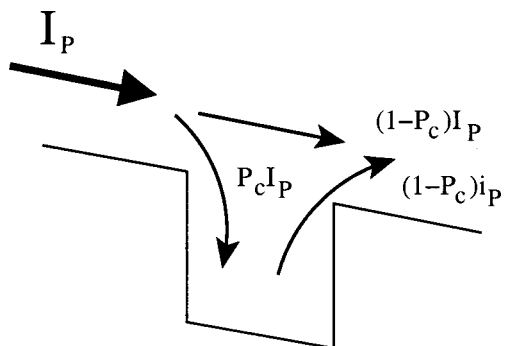


FIG. 2. Schematic band diagram of a unit gain single well in a QWIP including the total net photocurrent I_p and the emitted photocurrent by a single well.

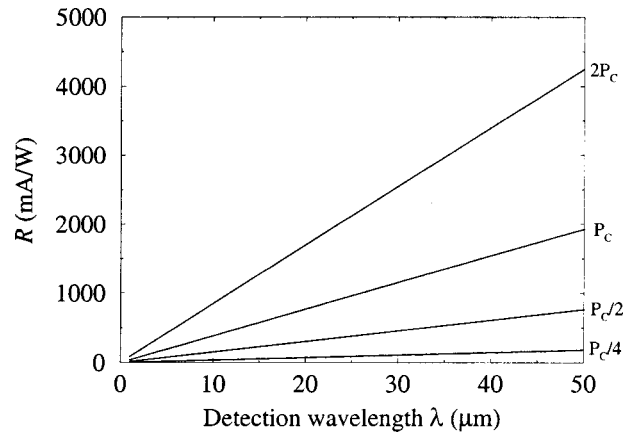


FIG. 3. Responsivity vs detection wavelength for a range of capture probabilities P_c that are independent of λ . The reference value for P_c of 0.346 was taken from Ref. 12.

$$g = \frac{1 - P_c}{P_c} \frac{1}{N} \tag{3}$$

as deduced by Levine *et al.*,^{7,10}

III. RESPONSIVITY

The responsivity of a QWIP is a commonly used figure-of-merit for detector performance and is defined as the photocurrent per unit watt of incident light,⁹ i.e.,

$$R = \frac{e \eta g}{h \nu}, \tag{4}$$

now

$$\nu = \frac{c}{\lambda},$$

thus, in terms of wavelength λ :

$$R = \frac{e \eta g}{hc} \lambda. \tag{5}$$

Taking the photoconductive gain g from Eq. (3), then

$$R = \frac{e \eta}{hc} \lambda \frac{1 - P_c}{P_c} \frac{1}{N}. \tag{6}$$

Using this expression, Fig. 3 illustrates the responsivity R as a function of detection wavelength λ , for various, but fixed, capture probabilities P_c . It can be seen that there is a direct proportionality between R and λ . The standard capture probability P_c of 0.346 was taken from the 5 μm $\text{Si}_{0.64}\text{Ge}_{0.36}/\text{Si}$ QWIP of Ref. 12, and the absolute values of the responsivity η of 10% which is typical of many n - and p -type devices.^{7,12,13} The number of wells in Fig. 3 was fixed at $N = 10$.

IV. CAPTURE PROBABILITY

Figure 4 shows the results of calculations¹⁴ of the detection wavelength λ versus the quantum well width l_w for a

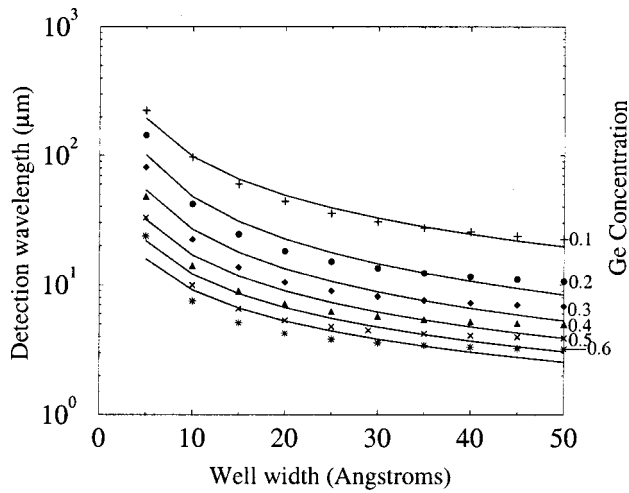


FIG. 4. Detection wavelength λ vs well width l_w for different Ge concentration with fitted curves.

series of $\text{Si}_{1-x}\text{Ge}_x/\text{Si}$ quantum wells. The solid lines show curves fitted via A and B to the data of the form

$$\lambda = \frac{A}{l_w^B} \tag{7}$$

It was found that the exponent B was always very close to 1, thus for the purpose of this work

$$\lambda = \frac{A}{l_w} \tag{8}$$

with the parameter A (having the dimensions of cm^2) depending on the depth (in this case, the Ge concentration x) of the well. The $\text{Si}_{0.64}\text{Ge}_{0.36}/\text{Si}$ QWIP¹² mentioned earlier, is to be used as an example device configuration. For this material concentration, it was found that the constant A linking the wavelength λ and the quantum well width l_w [as in Eq. (8)] was $2.248 \times 10^{-10} \text{ cm}^2$. The $\text{GaAs}/\text{Ga}_{0.74}\text{Al}_{0.26}\text{As}$ material system employed in the QWIPs of Ref. 15 will also be used. In this case A was found to be $4.83 \times 10^{-10} \text{ cm}^2$.

In the previous section the capture probability was assumed to have no dependence on λ , however, it would be expected in practice that the capture probability increases with increasing well width, as illustrated with the aid of the arrow thickness in each well in Fig. 5. There are two impor-

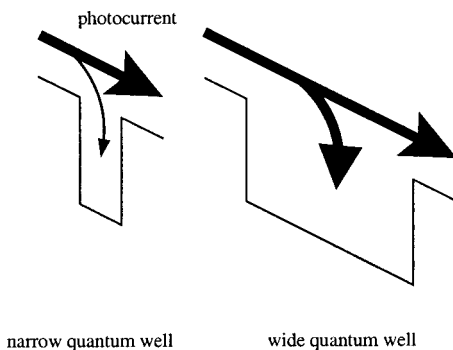


FIG. 5. Schematic illustration of the proportion of the photocurrent which is captured by subsequent quantum wells.

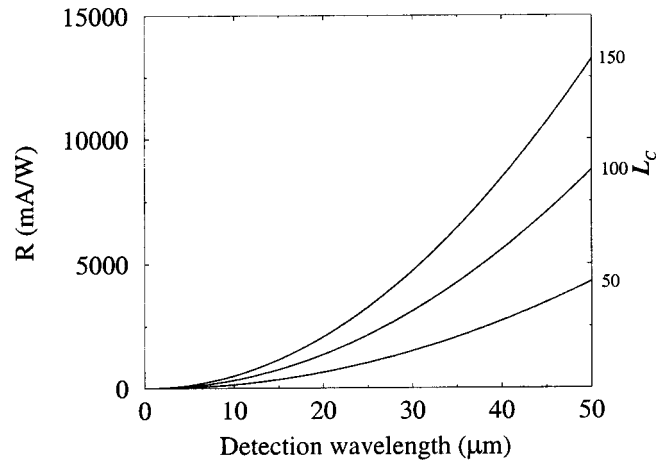


FIG. 6. Responsivity as a function of detection wavelength for a varying capture probability ($L_c=50,100,150 \text{ \AA}$) as defined in Eq. (10). The other parameters are from Ref. 12, $N=10$, and $A=2.248 \times 10^{-10} \text{ cm}^2$ for a Ge concentration of $x=0.3$ with the quantum efficiency η kept constant at 0.10.

tant limits

$$P_c \rightarrow 0 \text{ as } l_w \rightarrow 0$$

and

$$P_c \rightarrow 1 \text{ as } l_w \rightarrow \infty.$$

Both of these limits could be fitted empirically by taking the capture probability as

$$P_c = 1 - \exp\left(\frac{-l_w}{L_c}\right), \tag{9}$$

where L_c is a decay constant defining the rate of increase of the capture probability P_c with well width l_w . Using the expression for the wavelength dependence on the well width [Eq. (8)], then the capture probability can be expressed in terms of λ , i.e.,

$$P_c = 1 - \exp\left(\frac{-A}{L_c \lambda}\right). \tag{10}$$

Now substituting Eq. (10) into Eq. (6) gives a relationship between the responsivity and the detection wavelength which includes this simple model for the capture probability. Thus, the responsivity becomes

$$R = \frac{e \eta}{hcN} \lambda \frac{\exp\left(\frac{-A}{L_c \lambda}\right)}{1 - \exp\left(\frac{-A}{L_c \lambda}\right)}. \tag{11}$$

With the aid of Eq. (11), Fig. 6 replots the data of Fig. 3 (with the capture probability P_c scaled so that $P_c=0.346$ when $\lambda=5 \mu\text{m}$) to display R as a function of λ for several of the lengths L_c . It can be seen that the responsivity *increases* superlinearly with detection wavelength. This is because under this model the capture probability decreases with increasing wavelength, thus increasing the photoconductive gain g .

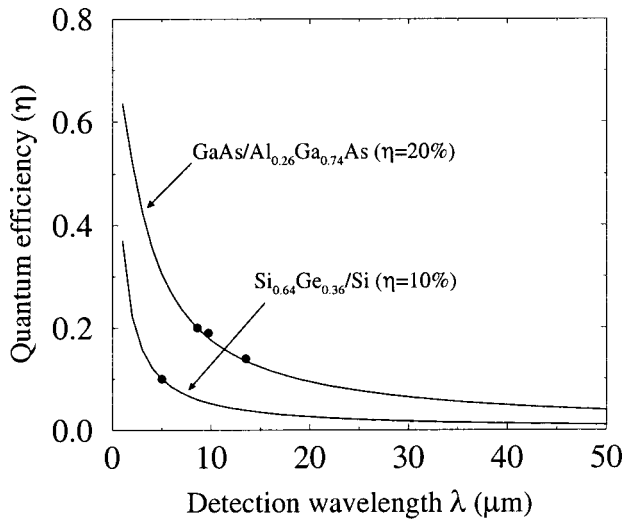


FIG. 7. Quantum efficiency as a function of detection wavelength for the example material systems (see Refs. 12 and 15).

V. QUANTUM EFFICIENCY

To improve the model still further, focus is now redirected towards the well quantum efficiency η which has been taken as constant. In Ref. 11, this quantum efficiency is defined as

$$\eta = P(1-r)[1 - \exp(-B\alpha l_w)], \tag{12}$$

where P is a polarization dependent constant ($P=1$ for p -type QWIPs), α is the absorption coefficient and B is a constant depending on the number of paths the infrared radiation made through the QWIP active region. In the worst case of a semiconductor/air reflection coefficient $r=1/3$ and $B=1$, the quantum efficiency η would become

$$\eta = \frac{2}{3}[1 - \exp(-\alpha N l_w)], \tag{13}$$

where, in an N well device, $N l_w$ is the total width of absorbing material. Using the relationship between the well width and the detection wavelength given in Eq. (8), we get

$$\eta = \frac{2}{3} \left(1 - \exp \left[-\alpha N \frac{A}{\lambda} \right] \right). \tag{14}$$

The absorption coefficient α depends on the material system and the doping density. From Ref. 12, we obtain $\alpha = 36.15 \times 10^3 \text{ cm}^{-1}$ for those particular 10 Si_{0.64}Ge_{0.36}/Si quantum wells which are homogeneously doped with boron giving a sheet concentration of $p_s = 1.2 \times 10^{12} \text{ cm}^{-2}$. Whereas, from Ref. 15 $\alpha = 25.4 \times 10^3 \text{ cm}^{-1}$ for the 25 period GaAs/Al_{0.26}Ga_{0.74}As QWIP with a doping density $N_D = 1.4 \times 10^{18} \text{ cm}^{-3}$ and surface grating to allow normal incidence. Then, substituting these values into Eq. (14), we obtain the η curves shown in Fig. 7. Then, returning to Eq. (11) we calculated the effect of the wavelength dependent quantum efficiency η summarized in Eq. (14) upon the responsivity-versus-wavelength relationship, but this time reverting back to the case of constant capture probability (see Fig. 8). The model assumes that the peak absorption coefficient is constant for all devices made from the same material, regardless of their absorption wavelength. In fact, the absorption coef-

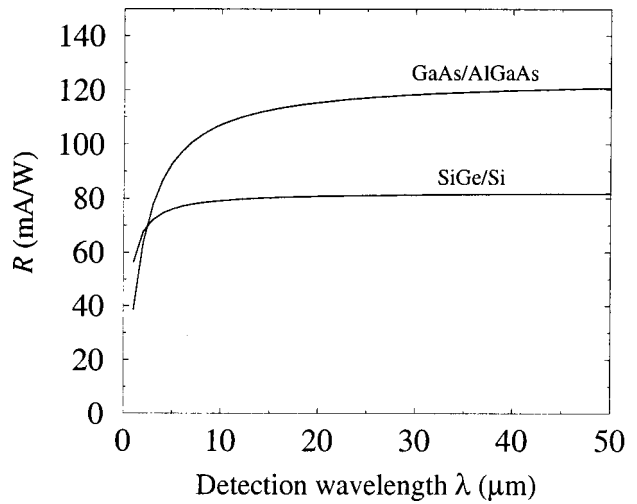


FIG. 8. Responsivity as a function of detection wavelength for a constant capture probability and a variable quantum efficiency in SiGe/Si and GaAs/AlGaAs quantum wells. $L_c = 150 \text{ \AA}$.

icient depends on the doping density, so for a constant doping density within the quantum wells, the absorption coefficient would become a function of the well width l_w and, hence, it would also be a function of the detection wavelength λ . For generality and to remove an additional variable from the analysis, the assumption is made that a series of devices could be designed to have the same absorption coefficient. This would be achieved by increasing the doping density as the width of the quantum wells is decreased—in order to achieve the same *sheet* density of carriers.

VI. COMPLETE MODEL

Figure 9 shows the behavior of the responsivity when both the capture probability and the quantum efficiency are allowed to be functions of the detection wavelength. We substituted Eq. (14) into Eq. (11) as shown in Eq. (15), thus completing the model

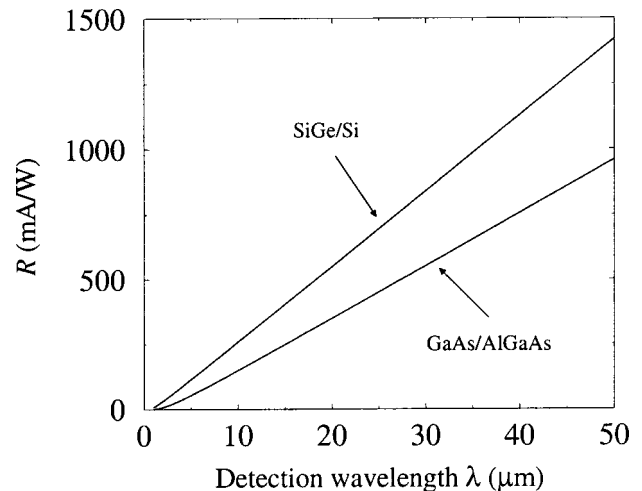


FIG. 9. Responsivity as a function of detection wavelength for a variable capture probability and quantum efficiency (as a function of detection wavelength). $L_c = 150 \text{ \AA}$.

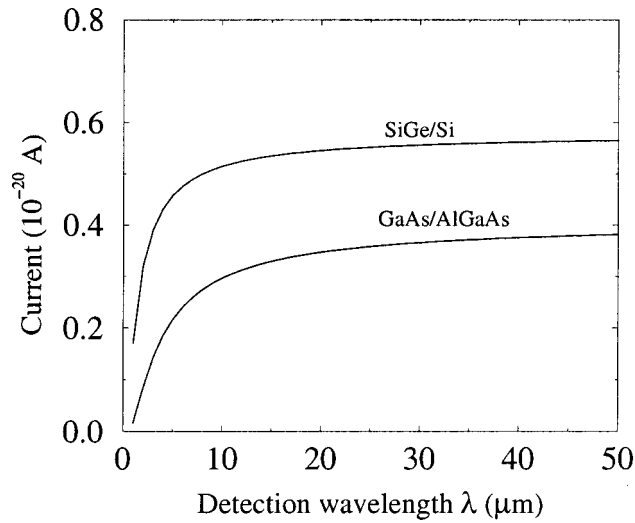


FIG. 10. Photocurrent as a function of detection wavelength when the power is 1 photon per second. $N_p=1$.

$$R = \frac{e}{hcN} \lambda \frac{\exp\left(\frac{-A}{L_c\lambda}\right)}{1 - \exp\left(\frac{-A}{L_c\lambda}\right)} \frac{2}{3} \left(1 - \exp\left[-\alpha N \frac{A}{\lambda}\right]\right). \quad (15)$$

In Fig. 9 we took $A=2.248 \times 10^{-10}$ cm² and $N=10$ as for the SiGe devices of Ref. 12 and $A=4.83 \times 10^{-10}$ cm² and $N=25$ as for the GaAs/AlGaAs devices of Ref. 15. It can be seen that there is almost a direct proportionality, mirroring the simple constants-based model at the beginning of this work. However, the absolute magnitudes of the responsivity are now more justified. Further consideration needs to be given to this data because although the responsivity increases with detection wavelength, it does not tell the full story. The unit of the responsivity is milliamps per watt with the latter representing the incident power. As the detection wavelength increases the photon energy decreases, hence, there are more photons per watt, which may be expected to produce more photoelectrons and thus more photocurrent.

In effect

$$R = \frac{I_p}{P},$$

where I_p is defined in Eq. (2) and the incident power is

$$P = N_p h\nu = N_p \frac{hc}{\lambda}.$$

N_p is the number of photons per second. Hence, the complete photocurrent I_p equation becomes

$$I_p = RP = N_p \frac{e}{N} \frac{\exp\left(\frac{-A}{L_c\lambda}\right)}{1 - \exp\left(\frac{-A}{L_c\lambda}\right)} \frac{2}{3} \left(1 - \exp\left[-\alpha N \frac{A}{\lambda}\right]\right). \quad (16)$$

Figure 10 shows the photocurrent per incident photon ($N_p=1$) as expressed in Eq. (16).

This is perhaps more vividly illustrated in Fig. 11 where

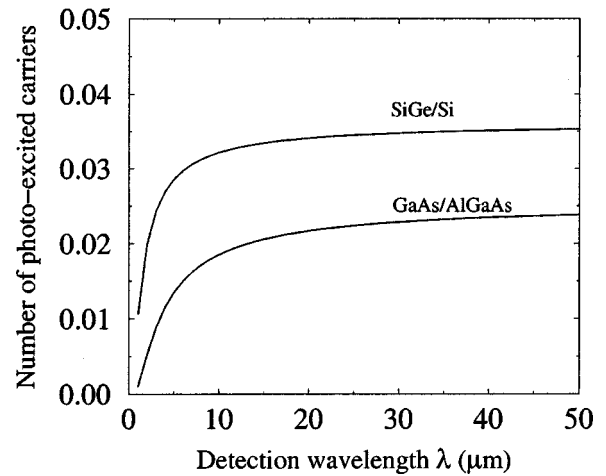


FIG. 11. The number of photoexcited electrons as a function of detection wavelength when the power is 1 photon per second.

the current is now given in terms of the number of photoexcited electrons per second

$$\text{Number of photoexcited electrons} = \frac{I_p}{1.6 \times 10^{-19} \text{ C}}. \quad (17)$$

Both figures show that in these terms the sensitivity of the QWIPs reaches a plateau and for increasing wavelength a constant number of electrons can be expected to be photoexcited per incident photon. (It maybe disconcerting to see SiGe QWIPs with 10% quantum efficiency having higher responsivity than 20% efficient GaAs/AlGaAs QWIPs. No significance should be attached to this, because the devices have different numbers of quantum wells and different doping densities, etc.)

VII. CONCLUSION

This article has derived two essential relationships for the capture probability and the quantum efficiency, each one as a function of the detection wavelength. These dependencies have enabled the responsivity to be expressed in terms of the detection wavelength. Subsequently, a photocurrent model was established by focusing on the remaining factor: the incident power (i.e., $P=I_p/R$). As the latter was restricted to the power of a single photon, then the number of photoexcited electrons (to produce the photocurrent) was determined. It was found that the number of photoelectrons per incident photon is likely to tend towards a constant as the wavelength of the incident light is increased beyond 10 μm and into the terahertz region of the spectrum. This is an encouraging result and suggests that far-infrared QWIPs may have a sensitivity no less than those in the midinfrared region. The realization of such devices will therefore be dependent upon the dark current in order to obtain a viable signal-to-noise ratio.^{14,16-19}

¹S. D. Gunapala *et al.*, *SPIE Conference on Infrared Detectors and Focal Plane Arrays V*, April 1998, p. 3379.

²S. Gunapala, G. Sarusi, J. Park, T. L. Lin, and B. Levine, *Phys. World* **7**, 35 (1994).

- ³P. Kruck, A. Weichselbaum, M. Helm, T. Fromherz, and G. Bauer, *Superlattices Microstruct.* **23**, 61 (1998).
- ⁴D. J. Robbins, M. B. Stanaway, W. Y. Leong, J. L. Glasper, and C. Pickering, *J. Mater. Sci.: Mater. Electron.* **6**, 363 (1995).
- ⁵B. F. Levine, *Semicond. Sci. Technol.* **8**, S400 (1993).
- ⁶C. H. Liu, *Appl. Phys. Lett.* **60**, 1507 (1992).
- ⁷B. F. Levine, *J. Appl. Phys.* **74**, R1 (1993).
- ⁸M. Ershov and H. C. Liu, *J. Appl. Phys.* **86**, 6580 (1999).
- ⁹K. K. Choi, *The Physics of Quantum Well Infrared Photodetectors* (World Scientific, Singapore, 1997).
- ¹⁰B. F. Levine, A. Zussman, S. D. Gunapala, M. T. Asom, J. M. Kuo, and W. S. Hobson, *J. Appl. Phys.* **72**, 4429 (1992).
- ¹¹*Handbook of Nanostructure Materials and Nanotechnology; Optical Properties*, edited by H. S. Nalwa (Academic, New York, 2000), Vol. 4.
- ¹²T. Fromherz, P. Kruck, M. Helm, G. Bauer, J. F. Nützel, and G. Abstreiter, *Appl. Phys. Lett.* **69**, 3372 (1996).
- ¹³R. People, J. C. Bean, G. C. Bethea, S. K. Sputz, and L. J. Peticolas, *Appl. Phys. Lett.* **61**, 1122 (1992).
- ¹⁴M. A. Gadir, P. Harrison, and R. A. Soref, *Superlattices Microstruct. Superlattices Microstruct.* **30**, 135 (2001).
- ¹⁵*Intersubband Transitions in Quantum Wells: Physics and Device Application I; Semiconductors and Semimetals*, edited by H. C. Liu and F. Capasso (Academic New York, 2000), Vol. 62.
- ¹⁶N. E. I. Etteh and P. Harrison, *IEEE J. Quantum Electron.* **37**, 672 (2001).
- ¹⁷N. E. I. Etteh and P. Harrison, *J. Appl. Phys.* (accepted for publication).
- ¹⁸N. E. I. Etteh and P. Harrison, *Physica E (Amsterdam)* (submitted).
- ¹⁹M. A. Gadir, P. Harrison, and R. A. Soref, *Physica E (Amsterdam)* (submitted).